The Cryosphere Discuss., https://doi.org/10.5194/tc-2018-3
Manuscript under review for journal The Cryosphere
Discussion started: 30 January 2018

The Cryosphere Discussions
Open Access
EGU

Modelled fracture and calving on the Totten Ice Shelf

Sue Cook[1], Jan Åström[2], Thomas Zwinger[2], Benjamin Keith Galton-Fenzi[3,1], Jamin Stevens Greenbaum[4], Richard Coleman[5,1]

[1] Antarctic Climate & Ecosystems Cooperative Research Centre, University of Tasmania, Hobart, Tasmania 7001, Australia.
[2] CSC - IT Center for Science, FI-02101 Espoo, Finland.
[3] Australian Antarctic Division, Kingston, Tasmania 7050, Australia.
[4] Institute for Geophysics, University of Texas at Austin, Austin, TX 78758, USA.
[5] Institute for Marine and Antarctic Studies, University of Tasmania, Hobart, Tasmania 7001, Australia.
Correspondence to: Sue Cook (sue.cook@utas.edu.au)

Abstract. The Totten Ice Shelf (IS) has a large drainage basin, much of which is grounded below sea level, leaving the glacier vulnerable to retreat through the Marine Ice Shelf Instability mechanism. The ice shelf has also been shown to be sensitive to changes in calving rate, as a very small retreat of the calving front from its current position is predicted to cause a change in flow at the grounding line. Therefore understanding the processes behind calving on the Totten IS is key to predicting its future sea level rise contribution. Here we use the Helsinki Discrete Element Model (HiDEM) to show that calving on the Totten IS is controlled not only by locally produced fractures at the calving front, but is also influenced by basal fractures which are likely produced at the grounding line. Our model results show that regrounding points may be key areas of basal crevasse production, and can produce basal crevasses in both an along and across flow orientation. As well as affecting calving, along flow basal crevasses at the grounding line may be a possible precursor to basal channels. We use two additional models to examine the evolution of basal fractures as they advect downstream, demonstrating that both strain and ocean melt have the potential to deform narrow fractures into the broad basal features observed near the calving front. The wide range of factors which influence fracture patterns and calving on this glacier will be a challenge for predicting its future mass loss.

1 Introduction

The calving of icebergs is responsible for around half of the mass lost from the Antarctic ice sheet (Depoorter et al., 2013; Liu et al., 2015; Rignot et al., 2013). Despite this, it is not currently well represented in the large scale ice sheet models, with

different calving approaches producing widely varying predictions of Antarctica's future sea level rise contribution (e.g. Deconto and Pollard, 2016; Levermann et al., 2014). Calving is ultimately controlled by how fractures develop on a glacier, and the key process involved can range from lateral rift propagation in the case of large icebergs, or the vertical penetration of a dense crevasse field in ice shelf disintegration (Benn et al., 2007). Fractures involved in calving may form in situ, or be advected into the calving front region from upstream. Basal crevasses have been observed near the grounding line of ice shelves (e.g. Bindschadler et al., 2011b; Jacobel et al., 2014) and may evolve in shape and size as they advect downstream (Jordan et al., 2014). To fully understand the calving behaviour of an ice shelf, we must therefore understand how fractures form and propagate on it. In this paper we applying fracture modelling to the Totten Ice Shelf (IS) to investigate these processes.

The Totten IS is fed by a large drainage basin, containing at least 3.5 m global sea level equivalent (Greenbaum et al., 2015). This region of the Antarctic Ice Sheet is grounded largely below sea level (Greenbaum et al., 2015), and has shown signs of significant grounding line fluctuation in the past (Aitken et al., 2016), leading to speculation that it may be vulnerable to Marine Ice Sheet Instability (Greenbaum et al., 2015; Pollard et al., 2015; Weertman, 1974). There have been some indications that the Totten IS may already have been thinning (Khazendar et al., 2013), although it is unclear if this represents a long term trend (Paolo et al., 2015). Crucially, the Totten IS has been identified as having one of the lowest proportions of "passive" ice in Antarctica (Fürst et al., 2016), i.e. the proportion of the ice shelf which can be lost without a resulting dynamic change in the grounded ice upstream. This means that any change in calving rate on the Totten IS could quickly cause an increased flux of ice across its grounding line and hence an increased contribution to global sea level rise.

The first stage to predicting future calving rates from Totten IS is to be able to reproduce current fracture patterns and calving rates. One tool which we can use to improve our understanding of the processes behind fracture and calving on ice shelves is a discrete element model (DEM). A DEM discretises the ice shelf geometry into a lattice of bonded particles. By allowing the bonds between particles to break, the model is able to explicitly develop fractures, rather than representing fracturing by a parameterisation as in continuum approaches. Discrete element models have been used successfully to simulate calving behaviour at marine terminating glaciers (Bassis and Jacobs, 2013; Vallot et al., 2017), to examine causes behind changes in calving behaviour (Åström et al., 2014) and to investigate how fracture propagation is affected by other elements of the cryospheric system (Benn et al., 2017; Vallot et al., 2017).

In this paper we present the first application of a discrete element model to an Antarctic ice shelf, and use it to examine fracture and calving on the Totten IS. We apply HiDEM to regions at both the calving front and the grounding zone to examine different areas of fracture formation. We also use a continuum ice flow model and a stochastic equation describing fracture development to examine how those fractures may evolve as they are advected downstream.

2 Data and Methods

2.1 Glaciological Data

The geometry of the model is taken from aerogeophysical data collected by the International Collaboration for Exploration of the Cryosphere through Aerogeophysical Profiling (ICECAP) project which has flown a dense network of flights of the Totten IS. The surface elevation (Blankenship et al., 2015) and ice thickness (Blankenship et al., 2012) data are interpolated using TELVIS (Thickness Estimation by a Lagrangian Validated Interpolation Scheme) (Roberts et al., 2011), to produce a geometry which is glaciologically self-consistent and has previously been used to infer basal melt rates on the glacier (Roberts et al., 2017). The bedrock elevation, which is used to distinguish zones of grounded/floating ice, is taken from gravity inversions (Greenbaum et al., 2015).

Model performance is evaluated by comparing the size and frequency of simulated icebergs with those observed in satellite images. The observed iceberg size distribution is calculated from three separate Landsat 7 images from 2009, 2010 and 2011, with each iceberg within 20 km of the calving front mapped and its area measured. The distance is chosen to ensure that only icebergs originating from the Totten IS are included.

2.2 Discrete Particle Model

We model fracture formation on Totten IS using the Helsinki Discrete Element Model (HiDEM) which is described in detail in Åström et al. (2013) and Riikilä et al. (2014). The model geometry is constructed with interconnected inelastic blocks, each representing a discrete volume of ice. The blocks are connected to their neighbours by breakable elastic beams whose energy dissipation depends on the deformation rate. As the ice deforms under its own weight, stresses on the beams increase; if stress reaches a failure threshold, the beam breaks creating a fracture in the modelled ice shelf. We have chosen a critical stress of approximately 1 MPa, governed by previous applications of the model to glacier ice (Åström et al., 2013, 2014).

The movement of each block of ice is calculated using a discrete version of Newton's equation of motion and is iterated with a timestep of 0.0001 s length. For computational reasons, we use a densely packed face-centred cubic (fcc) lattice of spherical blocks 50 m in size. The shape of the lattice introduces a weak directional bias in the elastic and fracture properties of the ice. The symmetry of the underlying fcc-lattice is however easily broken by the propagating cracks, as evidenced by the results. At the beginning of a fracture simulation, the ice is assumed to contain a small density of randomly scattered small pre-existing cracks. For these experiments, approximately 1% of the bonds are broken at the beginning of the simulation.

The effect of the surrounding ocean is simulated by applying a buoyancy force (F_b) to each block of ice forming the model domain:

$$F_b = (\rho_w - \rho_i) g V_p \,, \quad (1)$$

where ρ_w and ρ_i are the densities of ocean water and ice, g is the gravitational constant and V_p is the volume of a block. Since the model cannot cover the whole of the ice shelf due to computational cost, some of the boundaries of the domain are necessarily not simply floating passively, but are being pushed by the up-stream pressure from the land-based flowing part of the glacier. This pressure was modelled by applying hydrostatic pressure, P_{sc}, at the lateral boundaries of the simulated area where required.

$$P_{sc} = \begin{cases} \rho_i \, g \, z & z > 0 \\ (\rho_i - \rho_w) \, g \, z & z < 0 \end{cases}, \quad (2)$$

where z is the elevation above sea level. Where the model domain is grounded a constant basal friction F_f is applied:

$$F_f = -c \frac{dx}{dt}, \quad (3)$$

where $\frac{dx}{dt}$ is the sliding velocity and c is a drag coefficient set at 10^7.

2.3 Kardar-Parisi-Zhang (KPZ) Equation

To investigate the evolution of basal crevasses over time, we use two separate models to simulate the effects of basal melt and ice deformation. The first model simulates widening of basal cracks by ocean-driven melt in a simplistic fashion, by describing

The Cryosphere Discuss., https://doi.org/10.5194/tc-2018-3
Manuscript under review for journal The Cryosphere
Discussion started: 30 January 2018

the melting ice base as a propagating front. If melting is assumed spatially constant, the ice base will melt, as a first approximation, along the upward normal of its local surface. A generic model for such a front is the stochastic non-linear differential equation called the KPZ-equation (Kardar et al., 1986). The KPZ equation has been extensively used to describe, for example, slow combustion fronts or the growth bacterial colonies (e.g. Bonachela et al., 2011; Lam et al., 2017). The 1 dimensional KPZ equation reads:

$$\frac{\partial h(x,t)}{\partial t} = \nu \nabla^2 h(x,t) + \frac{\lambda}{2}[\nabla h(x,t)]^2 + F + \eta(x,t) \quad , \qquad (4)$$

where the vertical front location h varies with horizontal location x and time t. The first term on the r.h.s. can be thought of as a 'bending stiffness' that keeps the front from fluctuating too much, the second term drives the front perpendicular to its normal, F is the driving force (melting) and η is a stochastic term which can be used to introduce noise, but in this case we use to represent a series of initial basal crevasses to which the front propagation is applied.

2.4 Elmer/Ice

The effects of internal ice deformation will also change the shape of a basal fracture as it advects along with the ice shelf. To simulate how this may work we use the finite element model Elmer/Ice (Gagliardini et al., 2013) to simulate the changing shape of an idealised basal crevasse in two dimensions (2D).

The shelf is represented by a slab of ice initially 680 m thick and 4 km long, floating with neutral buoyancy, with an imposed basal crevasse 200 m wide at the base which penetrates 300 m vertically into the shelf (Fig. 5). Longitudinal stretching is simulated by fixing the left hand boundary of the domain, while moving the right hand side at 500 m/a. This is roughly equivalent to the maximum rate of stretching experienced on the Totten IS at the grounding line. The domain is iterated forward in time with timesteps of 12 hr, with the 2D velocity field solved at each time step using the Stokes equation together with Glen's flow law with an exponent of n=3 (see Gagliardini et al. (2013) for more detail). We choose a constant temperature within the ice of -9°C and no enhancement factor. The geometry of the domain is evolved with a kinematic condition for the free surface at the top and bottom boundaries, and is automatically adjusted to remain in hydrostatic equilibrium by maintaining the lower boundary at seawater pressure.

The Cryosphere Discuss., https://doi.org/10.5194/tc-2018-3
Manuscript under review for journal The Cryosphere
Discussion started: 30 January 2018

3 Results

3.1 Sources of fracture

The HiDEM model was run on two domains, one at the calving front and one near the grounding line. Our first model setup covers roughly 2000 km^2 of the Totten IS calving front (Fig. 1, 2). The area of the ice shelf covered in the calving front domain is almost entirely floating. The modelled fracture pattern shows tensile cracks, with the majority running roughly perpendicular to the calving front (Fig. 2b). These cracks appear where the calving front begins to spread laterally, as it is pushed towards the open sea by the upstream pressure. Observations of fracture patterns are hampered by thick snow cover on the Totten IS, however near the calving front similar cracks perpendicular to the calving front are clearly visible in satellite imagery (Fig. 2a). However, the large number of cracks visible perpendicular to the flow direction are not reproduced by the model. These across-flow features appear to be advected into the calving area from upstream. We hypothesise that these features originate at the grounding line, as basal crevassing at the grounding line has previously been observed on other ice shelves (e.g. Jacobel et al., 2014). These basal features would only become visible at the surface as they move downstream, where high melt rates and tensile acceleration of the ice cause the basal features to widen sufficiently to have a surface expression.

To test the hypothesis that the across-flow fractures develop at the grounding line, we use a second model domain covering a 45x45 km^2 section of ice at the southern-most point of the Totten IS (Fig. 1, 3). The observed geometry in this region shows a grounding zone rather than a distinct grounding line, where the ice re-grounds on many small islands (Fig. 3). In this region, the HiDEM simulation produces a number of fractures at the base of the ice shelf, which cluster around the re-grounding islands (Fig. 3). The formed cracks have a tendency to form either in the flow direction as shear cracks or in the cross-flow direction as tensile cracks. The cracks typically reach 200 m above the base of the ice. The fractures arise from the changes in stress at the base as the ice transitions from freely floating to grounded conditions. The across flow features are hypothesised to be the source of across flow surface features observed downstream on the Totten IS. It is possible that along flow basal crevasses could be a nucleus for the formation of basal channels, which subsequently grow by enhanced melting (Drews, 2015). This is a potential mechanism for the development of grounding-line sourced channels, the cause of which can be unclear in the absence of obvious subglacial hydrology (Alley et al., 2016).

The Cryosphere Discuss., https://doi.org/10.5194/tc-2018-3
Manuscript under review for journal The Cryosphere
Discussion started: 30 January 2018

3.2 Fracture advection

The basal crevasses formed in the grounding zone will undergo significant changes in shape as they advect downstream to the calving front. The glacier flow rate accelerates downstream of the grounding area, meaning the ice will stretch and thin, causing the basal cracks to widen as they move downstream. The water in the ocean cavity underneath the Totten IS is also known to be warm enough to drive melt of the ice (Gwyther et al., 2014; Rintoul et al., 2016; Roberts et al., 2017). As basal crevasses are exposed to sea water one might also expect that the cracks will become wider and deeper by melting.

To investigate the role of ocean melting we use the KPZ equation applied to a set of line cracks in a homogeneous 1 km thick glacier (Fig. 4). The vertical blue line segments at the bottom of the figure represent initial line cracks, represented by η in Equation 4. The melting front is then propagated forward in time with $\eta(t>0)=0$, and a driving force F that increases linearly along the flowline to represent the longer exposure to melt for downstream ice. The initial crack configuration ($\eta(x,0)$) is varied until a solution is found that approximates the measured base along the flight path. The surface elevation is thereafter calculated by assuming neutral buoyancy locally. In this way it is possible to reproduce both the surface and basal features of the Totten IS on an along-flow flight path (Fig. 4).

The evolution of basal fractures predicted here by the KPZ equation neglects spatial variations in melt rate across the ice shelf (e. g. Gwyther et al., 2014; Roberts et al., 2017), as well as variations in melt rate which have been predicted to occur within basal features (Jordan et al., 2014; Millgate et al., 2013). It also does not include the effects of internal ice deformation and strain thinning, which are particularly significant near the calving front where the ice shelf is unconfined and spreads laterally.

We separately investigate how internal ice deformation may affect the shape of basal crevasses using an idealised simulation in Elmer/Ice. The model uses an idealised domain with an initial narrow basal crevasse in a linear slab of ice, similar to the geometry used for the KPZ equation but this time with a single crack. Longitudinal stretching is imposed on the idealised ice shelf, by fixing the left hand boundary, while moving the right hand boundary horizontally. As the model runs forward over time, the longitudinal strain causes the initial crack to widen from 200 to 350 m (Fig. 5).

These experiments show that both longitudinal stretching and ocean melt within crevasses could lead narrow basal crevasses at the grounding line to evolve into broader features observed near the calving front of the Totten Glacier, as has previously

been suggested by Bassis and Ma (2015). Basal melt rates are highest at the southern end of the Totten Ice Shelf (Gwyther et al., 2014) where the thicker ice shelf means that the pressure dependent melting point is reduced at the base. Nearer the calving front, accelerating velocities and lateral spreading of the ice means internal deformation is more likely to be a dominant factor in basal crevasse evolution (e.g. Li et al., 2016).

With these results in mind, we introduce artificial basal features into the geometry of the original calving front model, to test if they can induce cracks perpendicular to the flow direction as observed in the terminus region. We mimic the observed features in Fig. 4 with straight, across-flow Gaussian-shaped basal features. Since the model domain was chosen to align with the dominant flow direction to improve computational efficiency, the introduced features also align with the model grid. The results of a HiDEM simulation are shown in Fig. 6. In this model realization, the Totten IS begins to form icebergs from fractures forming both parallel and perpendicular to the flow direction, as observed in satellite imagery (Fig. 2a). Without the introduction of across-flow basal features the terminus does not break apart easily, and fractures develop only slowly to form icebergs. Once the across-flow basal features are introduced into the model geometry, the HiDEM model produces icebergs much more quickly, although both simulations eventually reproduce the observed iceberg size distribution (Fig.7).

4 Conclusions

Our results represent the first application of a discrete element model, HiDEM, to an Antarctic ice shelf. We use the model to simulate fracture formation in two separate areas of the Totten IS. At the calving front, our results show that HiDEM reproduces fractures perpendicular to the calving front which drive the small, disintegration type calving events observed in satellite imagery. The model set-up at the calving front is not fully able to reproduce the fracture observed from satellite imagery, as it is missing many across-flow features which advect into the model domain from further upstream.

We suggest that these across-flow fractures develop at the grounding line, where the longitudinal stress caused by the transition from grounded to floating ice is likely to cause basal crevassing. A second HiDEM experiment around the southern-most grounding zone shows that high levels of basal crevassing occur particularly near to pinning points. Basal crevasses have previously been found at the grounding line around Antarctica (e.g. Jacobel et al., 2014) and our results suggest that pinning points are extremely important in determining where these fractures occur. The model predicts the formation of both across-

and along-flow basal crevasses at the grounding line, and it is possible that along-flow fractures may be a potential precursor for the basal channels observed on many ice shelves, the source of which is currently unclear (Alley et al., 2016).

As the across-flow basal crevasses advect downstream, ocean-driven melt and lateral spreading of the ice are likely to widen them, until they are large enough near the calving front to produce a visible surface expression. We have modelled the two effects separately, using the KPZ to simulate a spatially constant basal melt rate and a full-Stokes ice flow model (Elmer/Ice) to examine the effect of longitudinal stretching on basal crevasse shape. Using the KPZ equation to model the development of fractures under ocean melting, we demonstrate that broad across-flow basal features observed in aerogeophysical data can be reproduced by applying a spatially constant melt rate. Likewise, our Elmer/Ice simulation was able to produce a broadening of an initial narrow basal crevasse through longitudinal stretching. Both models make significant oversimplifications, but demonstrate that narrow features at the grounding line are a plausible source for the broader basal features advected into the calving zone.

Our results show that it is the interaction between the advected and locally produced fractures at the calving front which controls the shape of icebergs produced, and the speed with which they form. The development of fractures both at the grounding line and the calving front will be important in considering how calving rates may evolve in future. This presents a significant complication for accurately modelling calving at the Totten Glacier. The fracture pattern at the front depends not only on the local lateral spreading which creates along-flow rifts. It is also strongly affected by across-flow features which are likely produced at the grounding line. This implies that the conditions at the grounding line decades prior, as well as the cumulative ocean melt history on a section of ice shelf, will also have a significant impact on calving behaviour. The combination of multiple different effects is a significant challenge for calving models. One way to address this problem may be to combine modelling methods which allow local fractures to be accurately reproduced (e.g. HiDEM), in conjunction with traditional ice sheet modelling software which can track the history and advection of fractures over longer periods of time. Additionally, observations from satellite altimeters, such as CryoSat2, over ice shelf regions (Lacroix et al., 2007; Skourup et al., 2017) can also help give an improved understanding of surface crevasse characteristics, leading to improved modelling of fractures and calving.

Acknowledgements

Computing resources were provided by CSC – IT Center for Science Ltd. and National Computational Infrastructure grant m68. Data collection was supported through funding from NSF grants PLR-0733025 and PLR-1143843, NASA grants NNG10HPO6C and NNX11AD33G (Operation Ice Bridge and the American Recovery and Reinvestment Act), the Australian Government's Australian Antarctic Science Grant Program under projects AAS 3103, 4077 and 4346, the G. Unger Vetlesen Foundation, and the Jackson School of Geosciences. Our thanks to Dr. Jason Roberts, AAD for assistance in collating and processing data. This work was supported by the Australian Government's Business Cooperative Research Centres Programme through the Antarctic Climate and Ecosystems Cooperative Research Centre (ACE CRC)) and the Australian Research Council Special Research Initiative for Antarctic Gateway Partnership project.

References

Aitken, A. R. A., Roberts, J. L., Ommen, T. D. van, Young, D. A., Golledge, N. R., Greenbaum, J. S., Blankenship, D. D. and Siegert, M. J.: Repeated large-scale retreat and advance of Totten Glacier indicated by inland bed erosion, Nature, 533(7603), 385–389, doi:10.1038/nature17447, 2016.

Alley, K. E., Scambos, T. A., Siegfried, M. R. and Fricker, H. A.: Impacts of warm water on Antarctic ice shelf stability through basal channel formation, Nat. Geosci., 9(April), doi:10.1038/ngeo2675, 2016.

Åström, J. A., Riikilä, T. I., Tallinen, T., Zwinger, T., Benn, D., Moore, J. C. and Timonen, J.: A particle based simulation model for glacier dynamics, Cryosphere, 7(5), 1591–1602, doi:10.5194/tc-7-1591-2013, 2013.

Åström, J. A., Vallot, D., Schäfer, M., Welty, E. Z., O'Neel, S., Bartholomaus, T. C., Liu, Y., Riikilä, T. I., Zwinger, T., Timonen, J. and Moore, J. C.: Termini of calving glaciers as self-organized critical systems, Nat. Geosci., 7(12), 874–878, doi:10.1038/ngeo2290, 2014.

Bassis, J. N. and Jacobs, S.: Diverse calving patterns linked to glacier geometry, Nat. Geosci., 6(10), 833–836, doi:10.1038/ngeo1887, 2013.

Bassis, J. N. and Ma, Y.: Evolution of basal crevasses links ice shelf stability to ocean forcing, Earth Planet. Sci. Lett., 409, 203–211, doi:10.1016/j.epsl.2014.11.003, 2015.

Benn, D. I., Warren, C. R. and Mottram, R. H.: Calving processes and the dynamics of calving glaciers, Earth-Science Rev., 82(3–4), 143–179, doi:10.1016/j.earscirev.2007.02.002, 2007.

Benn, D. I., Åström, J. A., Zwinger, T., Todd, J., Nick, F. M., Cook, S., Hulton, N. R. J. and Luckman, A.: Melt-under-cutting and buoyancy-driven calving from tidewater glaciers: new insights from discrete element and continuum model simulations, J. Glaciol., 1–12, doi:10.1017/jog.2017.41, 2017.

Bindschadler, R., Choi, H. and ASAID Collaborators: High-resolution image-derived grounding and hydrostatic lines for the Antarctic Ice Sheet, [online] Available from: http://dx.doi.org/10.7265/N56T0JK2., 2011a.

Bindschadler, R., Vaughan, D. G. and Vornberger, P.: Variability of basal melt beneath the Pine Island Glacier ice shelf , West Antarctica, J. Glaciol., 57(204), 581–595, 2011b.

Blankenship, D. D., Kempf, S. D. and Young, D. A.: IceBridge HiCARS 2 L2 Geolocated Ice Thickness, Version 1, , Boulder, Colorado USA. NASA National Snow and Ice, doi:http://dx.doi.org/10.5067/9EBR2T0VXUDG., 2012.

Blankenship, D. D., Kempf, S. D., Young, D. A. and Lindzey, L. E.: IceBridge Photon Counting Lidar L1B Unclassified Geolocated Photon Elevations, Version 1, , Boulder, Colorado USA. NASA National Snow and Ice, doi:http://dx.doi.org/10.5067/U3E4Q5WWVSP9, 2015.

Bonachela, J. A., Nadell, C. D., Xavier, J. B. and Levin, S. A.: Universality in Bacterial Colonies, J. Stat. Phys., 144, 303–315, doi:10.1007/s10955-011-0179-x, 2011.

Deconto, R. M. and Pollard, D.: Contribution of Antarctica to past and future sea-level rise, Nature, 531(7596), 591–597, doi:10.1038/nature17145, 2016.

Depoorter, M. A., Bamber, J. L., Griggs, J. A., Lenaerts, J. T. M., Ligtenberg, S. R. M., van den Broeke, M. R. and Moholdt, G.: Calving fluxes and basal melt rates of Antarctic ice shelves., Nature, 502(7469), 89–92, doi:10.1038/nature12567, 2013.

Drews, R.: Evolution of ice-shelf channels in Antarctic ice shelves, Cryosph., 9(3), 1169–1181, doi:10.5194/tc-9-1169-2015, 2015.

Fürst, J. J., Durand, G., Gillet-Chaulet, F., Tavard, L., Rankl, M., Braun, M. and Gagliardini, O.: The safety band of Antarctic ice shelves, Nat. Clim. Chang., (6), 479–482, doi:10.1038/NCLIMATE2912, 2016.

Gagliardini, O., Zwinger, T., Gillet-Chaulet, F., Durand, G., Favier, L., De Fleurian, B., Greve, R., Malinen, M., Martín, C., Räback, P., Ruokolainen, J., Sacchettini, M., Schäfer, M., Seddik, H. and Thies, J.: Capabilities and performance of Elmer/Ice, a new-generation ice sheet model, Geosci. Model Dev., 6(4), 1299–1318, doi:10.5194/gmd-6-1299-2013, 2013.

Greenbaum, J. S., Blankenship, D. D., Young, D. A., Richter, T. G., Roberts, J. L., Aitken, A. R. A., Legrésy, B., Schroeder, D. M., Warner, R. C., van Ommen, T. D. and Siegert, M. J.: Ocean access to a cavity beneath Totten Glacier in East Antarctica, Nat. Geosci., 8, 6–10, doi:10.1038/NGEO2388, 2015.

Gwyther, D. E., Galton-Fenzi, B. K., Hunter, J. R. and Roberts, J. L.: Simulated melt rates for the Totten and Dalton ice shelves, Ocean Sci., 10(3), 267–279, doi:10.5194/os-10-267-2014, 2014.

Jacobel, R. W., Christianson, K., Wood, A. C., Dallasanta, K. J. and Gobel, R. M.: Morphology of basal crevasses at the grounding zone of Whillans Ice Stream, West Antarctica, Ann. Glaciol., 55(67), 57–63, doi:10.3189/2014AoG67A004, 2014.

Jordan, J. R., Holland, P. R., Jenkins, A., Piggott, M. D. and Kimura, S.: Modelling ice-ocean interaction in ice-shelf crevasses, J. Geophys. Res., 119, 2121–2128, doi:10.1002/jgrc.20224, 2014.

Kardar, M., Parisi, G. and Zhang, Y.-C.: Dynamic scaling of growing interfaces, Phys. Rev. Lett., 56(9), 889–892, 1986.

Khazendar, A., Schodlok, M. P., Fenty, I., Ligtenberg, S. R. M., Rignot, E. and van den Broeke, M. R.: Observed thinning of Totten Glacier is linked to coastal polynya variability., Nat. Commun., 4, 2857, doi:10.1038/ncomms3857, 2013.

Lacroix, P., Legrésy, B., Coleman, R., Dechambre, M. and Rémy, F.: Dual-frequency altimeter signal from Envisat on the Amery ice-shelf, Remote Sens. Environ., 109(3), 285–294, doi:10.1016/j.rse.2007.01.007, 2007.

Lam, F., Mi, X. and Higgins, A. J.: Front roughening of flames in discrete media, Phys. Rev., 96(1), 13107, doi:10.1103/PhysRevE.96.013107, 2017.

Levermann, A., Winkelmann, R., Nowicki, S., Fastook, J. L., Frieler, K., Greve, R. and Hellmer, H. H.: Projecting Antarctic ice discharge using response functions from SeaRISE ice-sheet models, Earth Syst. Dyn., 5, 271–293, doi:10.5194/esd-5-271-2014, 2014.

Li, X., Rignot, E., Mouginot, J. and Scheuchl, B.: Ice flow dynamics and mass loss of Totten Glacier, East Antarctica from 1989 to 2015, Geophys. Res. Lett., (May), doi:10.1002/2016GL069173, 2016.

Liu, Y., Moore, J. C., Cheng, X., Gladstone, R. M., Bassis, J. N., Liu, H., Wen, J. and Hui, F.: Ocean-driven thinning enhances iceberg calving and retreat of Antarctic ice shelves, Proc. Natl. Acad. Sci., 201415137, doi:10.1073/pnas.1415137112, 2015.

Millgate, T., Holland, P. R., Jenkins, A. and Johnson, H. L.: The effect of basal channels on oceanic ice-shelf melting, J. Geophys. Res., 118, 6951–6964, doi:10.1002/2013JC009402, 2013.

Paolo, F. S., Fricker, H. A. and Padman, L.: Volume loss from Antarctic ice shelves is accelerating, Science (80-.)., 348(6232), 327–332, doi:10.1126/science.aaa0940, 2015.

Pollard, D., Deconto, R. M. and Alley, R. B.: Potential Antarctic Ice Sheet retreat driven by hydrofracturing and ice cliff failure, Earth Planet. Sci. Lett., 412, 112–121, doi:10.1016/j.epsl.2014.12.035, 2015.

Rignot, E., Jacobs, S., Mouginot, J. and Scheuchl, B.: Ice-shelf melting around Antarctica, Science (80-.)., 341(6143), 266–270, 2013.

Riikilä, T. I., Tallinen, T., Åström, J. and Timonen, J.: A discrete-element model for viscoelastic deformation and fracture of glacial ice, Comput. Phys. Commun., (APRIL), 13–22, doi:10.1016/j.cpc.2015.04.009, 2014.

Rintoul, S. R., Silvano, A., Pena-molino, B., Wijk, E. Van, Rosenberg, M., Greenbaum, J. S. and Blankenship, D. D.: Ocean heat drives rapid basal melt of the Totten Ice Shelf, Sci. Adv., 2(12), e1601610, 2016.

Roberts, J., Galton-Fenzi, B. K., Paolo, F. S., Donnelly, C., Gwyther, D. E., Padman, L., Young, D., Warner, R., Greenbaum, J., Fricker, H. A., Payne, A. J., Cornford, S., Le Brocq, A. M., Van Ommen, T., Blankenship, D. D. and Siegert, M. J.: Ocean forced variability of Totten Glacier mass loss, Geol. Soc. Spec. Publ., 2017.

Roberts, J. L., Warner, R. C., Young, D., Wright, A., Ommen, T. D. Van, Blankenship, D. D., Siegert, M., Young, N. W., Tabacco, I. E., Forieri, A., Passerini, A., Zirizzotti, A. and Frezzotti, M.: Refined broad-scale sub-glacial morphology of Aurora Subglacial Basin , East Antarctica derived by an ice-dynamics-based interpolation scheme, Cryosph., 5, 551–560, doi:10.5194/tc-5-551-2011, 2011.

Skourup, H., Farrell, S. L., Hendricks, S., Ricker, R., Thomas, W., Armitage, K., Ridout, A., Andersen, O. B., Haas, C. and Baker, S.: An Assessment of State-of-the-Art Mean Sea Surface and Geoid Models of the Arctic Ocean : Implications for Sea Ice Freeboard Retrieval, JGR Ocean., 122(11), 8593–8613, 2017.

Vallot, D., Åström, J., Zwinger, T., Pettersson, R., Everett, A., Benn, D. I., Luckman, A., Pelt, W. J. J. Van and Nick, F.: Effects of undercutting and sliding on calving : a coupled approach applied to Kronebreen , Svalbard, Cryosph. Discuss., doi:doi.org/10.5194/tc-2017-166, 2017.

Weertman, J.: Stability of the junction of an ice sheet and an ice shelf, J. Glaciol., 13(67), 3–11, 1974.

The Cryosphere Discuss., https://doi.org/10.5194/tc-2018-3
Manuscript under review for journal The Cryosphere
Discussion started: 30 January 2018

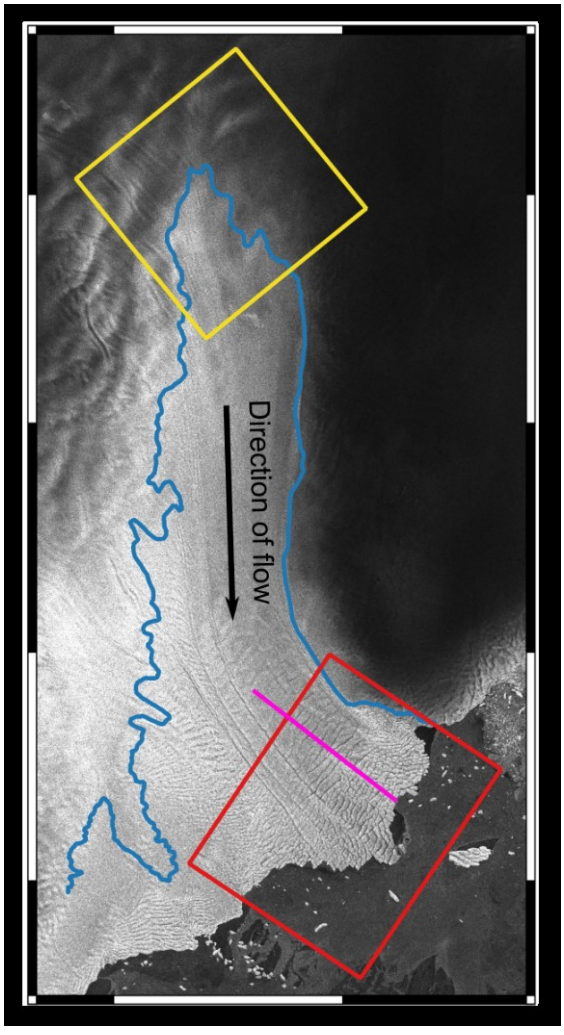

Figure 1: Locations of model domains. Blue line shows the grounding line as defined by ASAID (Bindschadler et al., 2011a). Red box shows extent of HiDEM calving front model. Yellow box shows extent of HiDEM grounding line model. Pink line shows flight path used to tune the KPZ model. Background image: Sentinel 1, December 2016.

The Cryosphere Discuss., https://doi.org/10.5194/tc-2018-3
Manuscript under review for journal The Cryosphere
Discussion started: 30 January 2018

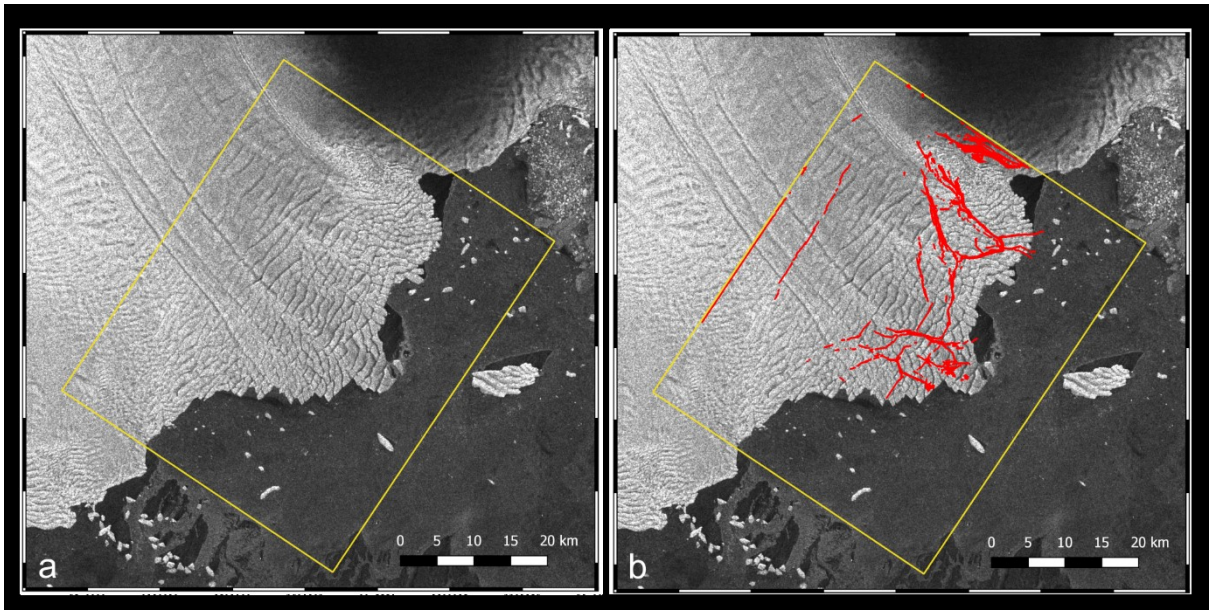

Figure 2: Observed and modelled fractures. a. Location of calving front domain (yellow box). Back ground image from Sentinel 1 (December 2016) shows the dense pattern of fractures at the calving front **b.** Model output from HiDEM at calving front. Red dots show modelled crevasses. Crevasses largely run parallel to flow/perpendicular to calving front.

The Cryosphere Discuss., https://doi.org/10.5194/tc-2018-3
Manuscript under review for journal The Cryosphere
Discussion started: 30 January 2018

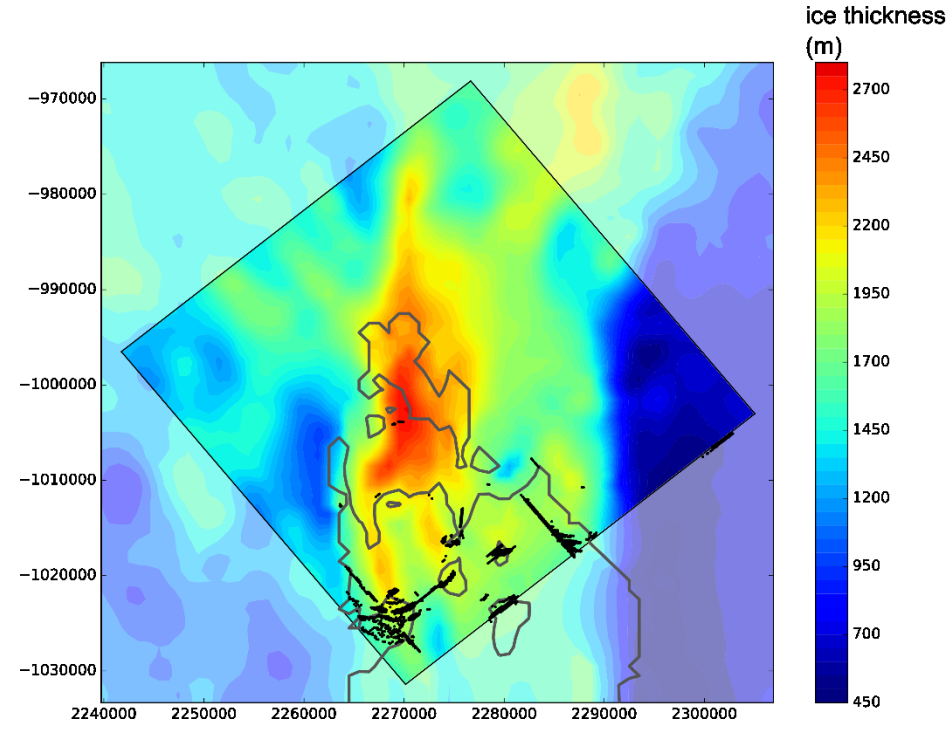

Figure 3: Model output from HiDEM at the grounding zone. Black dots show modelled crevasses. Grey line shows grounding line from HiDEM model geometry. Background colour shows ice thickness. Crevasses are clustered around pinning points where the ice regrounds.

5

The Cryosphere Discuss., https://doi.org/10.5194/tc-2018-3
Manuscript under review for journal The Cryosphere
Discussion started: 30 January 2018

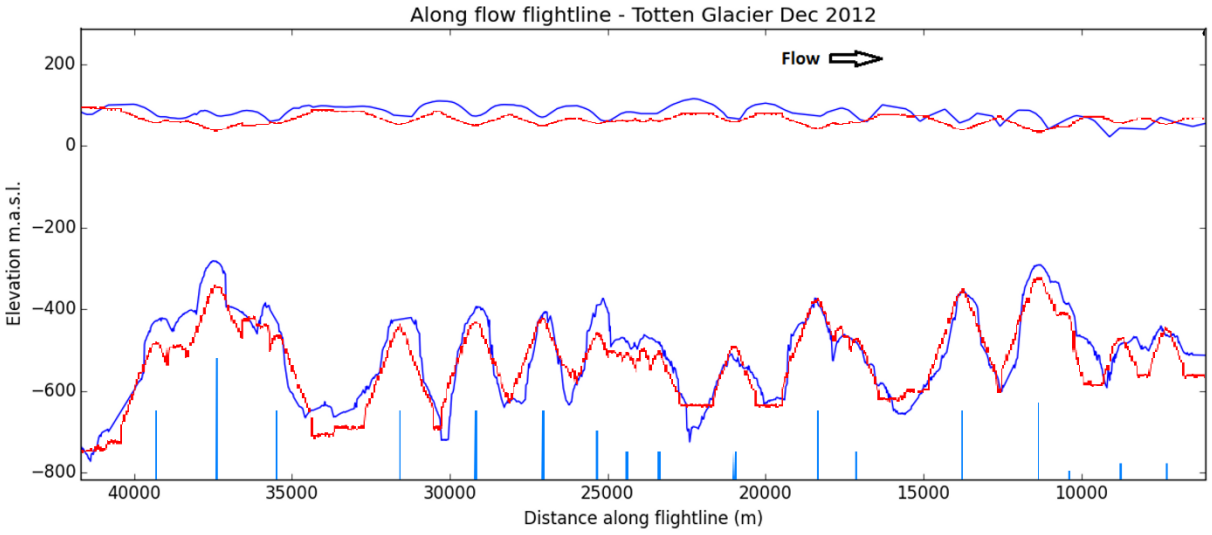

Figure 4: Development of basal fracture geometry under ocean melt. Measured (dark blue) and computed (red) ice surface and base along flight line. Vertical lines at the bottom of the figure represent relative position and height of original basal fractures.

The Cryosphere Discuss., https://doi.org/10.5194/tc-2018-3
Manuscript under review for journal The Cryosphere
Discussion started: 30 January 2018

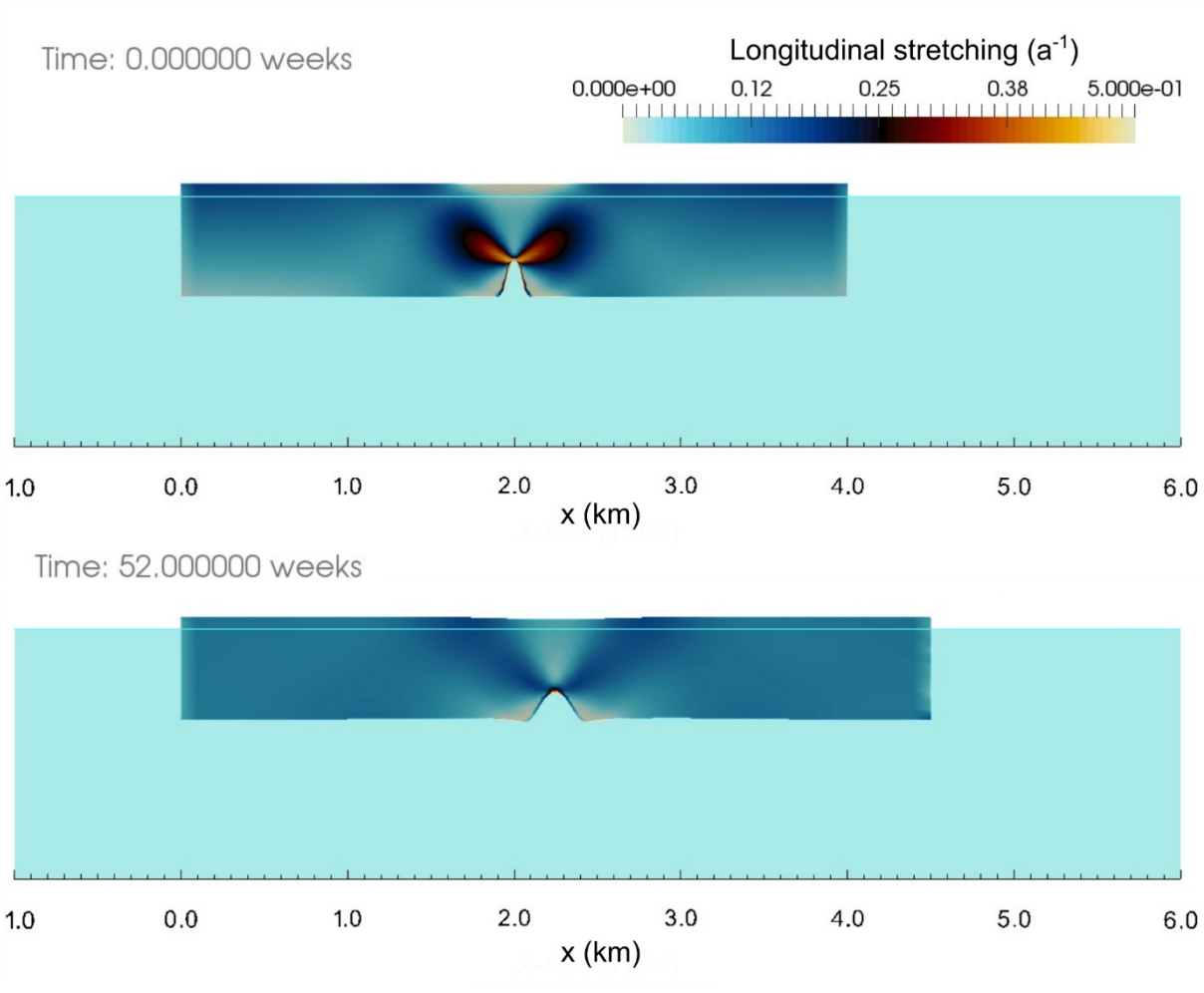

Figure 5: Evolution of basal crevasse geometry in Elmer/Ice. Top panel shows initial geometry of basal crevasse experiment. Bottom panel shows evolved geometry under longitudinal stretching after one year. The effect of longitudinal stretching on the shelf widens the basal crevasse.

The Cryosphere Discuss., https://doi.org/10.5194/tc-2018-3
Manuscript under review for journal The Cryosphere
Discussion started: 30 January 2018

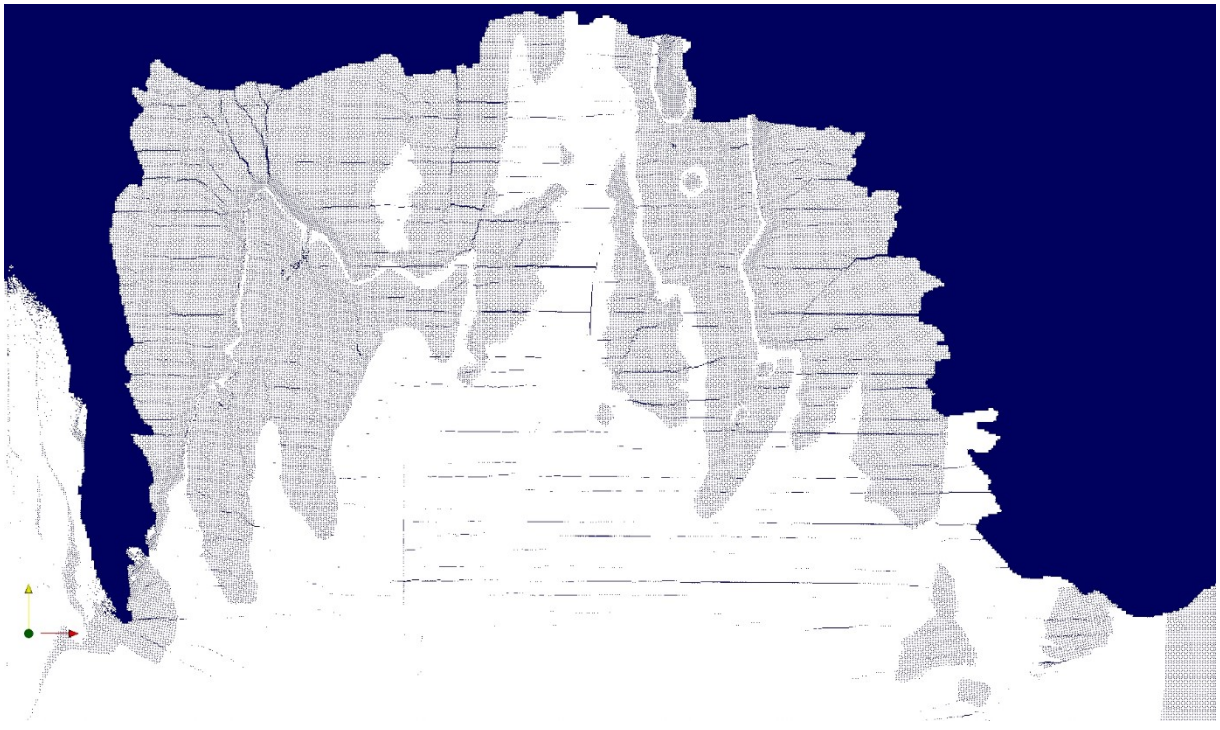

Figure 6: Fracture pattern with additional basal features. Example output from the HiDEM model on the Totten IS, showing modelled fracture pattern. Light scattering within the ice and fractures are computed to show internal structure. The introduced basal features are a source of additional across flow fracture, producing a checkerboard fracture pattern similar to observation.

The Cryosphere Discuss., https://doi.org/10.5194/tc-2018-3
Manuscript under review for journal The Cryosphere
Discussion started: 30 January 2018

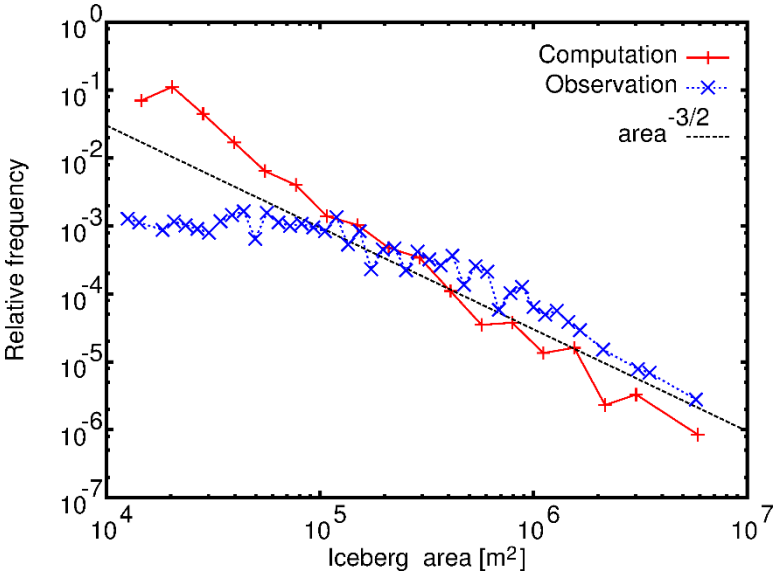

Figure 7. Evaluation of HiDEM results. Frequency distribution of simulated and observed iceberg sizes. The model is able to reproduce the observed size distribution. The disparity at smaller iceberg sizes is caused by difficulty of detection in satellite imagery.